BIBLIOGRAPHIC INFORMATION SYSTEM

JOURNAL FULL TITLE: Journal of Biomedical Research & Environmental Sciences
ABBREVIATION (NLM): J Biomed Res Environ Sci **ISSN:** 2766-2276 **WEBSITE:** https://www.jelsciences.com

SCOPE & COVERAGE

- **Sections Covered:** 34 specialized sections spanning 143 topics across Medicine, Biology, Environmental Sciences, and General Science
- Ensures broad interdisciplinary visibility for high-impact research.

PUBLICATION FEATURES

- **Review Process:** Double-blind peer review ensuring transparency and quality
- **Time to Publication:** Rapid 21-day review-to-publication cycle
- **Frequency:** Published monthly
- **Plagiarism Screening:** All submissions checked with iThenticate

INDEXING & RECOGNITION

- **Indexed in:** Google Scholar, IndexCopernicus (**ICV 2022: 88.03**)
- **DOI:** Registered with CrossRef (**10.37871**) for long-term discoverability
- **Visibility:** Articles accessible worldwide across universities, research institutions, and libraries

OPEN ACCESS POLICY

- Fully Open Access journal under Creative Commons Attribution 4.0 License (CC BY 4.0)
- Free, unrestricted access to all articles globally

GLOBAL ENGAGEMENT

- **Research Reach:** Welcomes contributions worldwide
- **Managing Entity:** SciRes Literature LLC, USA
- **Language of Publication:** English

SUBMISSION DETAILS

- Manuscripts in Word (.doc/.docx) format accepted

SUBMISSION OPTIONS

- **Online:** https://www.jelsciences.com/submit-your-paper.php
- **Email:** support@jelsciences.com, support@jbresonline.com

HOME ABOUT ARCHIVE SUBMIT MANUSCRIPT APC

Vision: The Journal of Biomedical Research & Environmental Sciences (JBRES) is dedicated to advancing science and technology by providing a global platform for innovation, knowledge exchange, and collaboration. Our vision is to empower researchers and scientists worldwide, offering equal opportunities to share ideas, expand careers, and contribute to discoveries that shape a healthier, sustainable future for humanity.

JOURNAL OF BIOMEDICAL RESEARCH & ENVIRONMENTAL SCIENCES
ISSN: 2766-2276
SUBJECT AREA(S): PHYSICS
DOI: 10.37871

RESEARCH ARTICLE

The Occluded Electron

Munawar Karim[1*] and Ashfaque H Bokhari[2]

1Department of Biology, Chemistry and Physics, Faculty of Natural and Applied Sciences Namibia University of Science and Technology, Windhoek, Namibia

2Department of Mathematics and Statistics, King Fahd University of Petroleum and Minerals, Dhahran, Saudia Arabia

Abstract

We include effects of self-gravitation in the self-interaction of single electrons with the vacuum electromagnetic field. When the effect of gravitation is included there is an inevitable cut-off of the k-vector - the upper limit is finite. The inward pressure of the self-gravitating field balances the outward pressure of self-interaction. Both pressures are generated by self-interactions of the electron with two fields - the vacuum electromagnetic field and the self-induced gravitational field. Specifically we demonstrate that gravitational effects must be included to stabilize the electron. We use the Einstein equation and equations of hydrostatic equilibrium to perform an exact calculation of the bare mass and electron radius. In the closed-form solution we find the electron radius to be $r_e = \sqrt{\alpha/4\pi}\sqrt{\hbar G/c^3} = \sqrt{\alpha/4\pi}\, l_P \approx 4\times10^{-37} m$. $\sqrt{\hbar G/c^3}$ is the Planck length ℓ_P , which is educed from first principles. The radius is independent of $\hbar$, it depends on k and k The elecron mass is $=(1/2)\sqrt{\alpha/4\pi}\, m_P$ in terms of the Planck mass m_P. We find that the electromagnetic and gravitational fields merge at $\mu_* = \sqrt{\alpha/4\pi}\sqrt{\hbar c/G} = (1/2)\sqrt{\alpha/4\pi}\, m_P = 10^{17} GeV$ in terms of the Planck mass m_P. Since the unified field is independent of $\hbar$ (it depends on e and G alone) we conclude that it is continuous. We extend our result to calculate the pressure profile within the electron. We present both numerical, and analytical calculations based on approximations. We also calculate the speed of excitations within the electron which display two distinct regions; a hard shell surrounding a softer core. We also provide an explanation for the large discrepancy between the theoretical and measured mass of electrons.

PACS 04.62.+ v, 11.10.Gh, 12.10.-g, 12.20.Ds

Introduction

The paradox of electron stability has been recognized since its discovery [1]. Instability is inevitable in any system with charge distributed over an extended volume. There have been several conjectures to explain stability (i) a shell of non-electromagnetic origin to contain the field (Poincare' stress), (ii) using radiation reaction to compensate the outward pressure (Abraham-Lorentz equation), (iii) dimensional regularization etc.

***Corresponding author(s)**

Munawar Karim, Department of Biology, Chemistry and Physics, Faculty of Natural and Applied Sciences, Namibia University of Science and Technology, Windhoek, Namibia

Email:
mkarim@icloud.com

DOI: 10.37871/jbres2301

Submitted: 26 July 2025

Accepted: 25 May 2026

Published: 26 May 2026

How to cite this article: Karim M, Bokhari AH. The Occluded Electron. J Biomed Res Environ Sci. 2026 May 26; 7(5): 13. Doi: 10.37872/jbres2302

Poincare's suggestion was to trap the charge in a rigid shell subjecting it to a stress [2]. This was found to be untenable.

When radiation reaction is included as in the Abraham-Lorentz equation [3], one gets runaway solutions instead of stability.

Yet another suggestion was to treat the space dimension as a free parameter *d* (dimensional regularization) [4], then use its variation to solve a divergent integral. Choosing *d*=4 unfortunately leads to a pole, which then must be compensated, raising new issues.

It was recognized that renormalisation was required to compute the self-energy of the electron. In this scheme the measured mass of electrons *m* was used to terminate the divergence.

With the advent of quantum electrodynamics new schemes were proposed, but even these were partially successful. Although the calculations are well-established, the result is inevitably divergent (albeit logarithmically at best). Various work-arounds have been proposed, among them a modification of electrodynamics at short distances, terminating the integral at the Compton or Planck length etc. We will discuss some of these later.

These approaches have one common motivation: that infinities are a mathematical anomaly which must be side-stepped, removed, truncated or at worst ignored. Needless to say these approaches suffer from deficiencies. Infinities remain because they are intrinsic to the theory.

We claim instead that the appearance of infinities is the consequence of ignoring basic physical phenomena. The infinities are real. In the sections below we describe what these are and calculate the resulting corrected mass from first principles.

Computation algorithm

Using standard quantum electrodynamics to calculate the mass shift for a free electron, Feynman's final result is

$$\Delta m = \frac{4\pi e^2}{2mi}\int_{-\infty}^{\infty} \frac{\tilde{u}(2m+2k)u}{k^2 - 2\vec{p}\cdot\vec{k}} \frac{d^4k}{(2\pi)^4}\frac{1}{k^2} \qquad (1)$$

for the mass correction Δm [5] where m is the experimental mass and e the charge of the electron ; the variables are k and p, the four-momenta of photons and p the electron.

The integral being of the form d^4k/k^4 is intrinsically divergent. Feynman obviates the divergence by modifying the photon kernel. The effect is to alter the laws of electrodynamics at short distances. Although no reason exists to justify this alteration, since there is no evidence that the laws of electrodynamics are inadequate at short distances. Even so with this alteration the integral is logarithmically divergent; it also necessitates the introduction of a free parameter. The puzzle remains unsolved.

The diagram figure 1 represents the electron emitting and absorbing a single photon. ft bpFU3.5051in1.4382in0ptElectron emitting and absorbing a virtual photon. Figure 1 feynmanoneloop.pnglanguage "Scientific Word";type "GRAPHIC";maintain-aspect-ratio TRUE;display "USEDEF";valid_file "F";width 3.5051in;height 1.4382in;depth 0pt;original-width 3.4584in;original-height 1.4027in;cropleft "0";croptop "1";cropright "1";cropbottom "0";filename 'C:/Users/mkari/OneDrive/Documents/FeynmanOneloop.png';file-properties "XNPEU". [6].

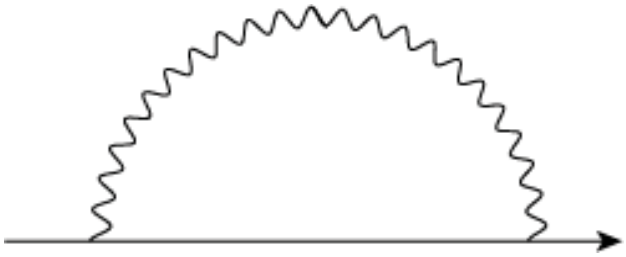

Figure 1 Schematic representation of the semicircular oscillatory trajectory of a charged particle moving along a horizontal reference axis under varying electric field conditions.

Near field

A way out of this dilemma is to re-interpret the one-loop correction and relate it to fields in the vicinity of a classical radiation source. Surrounding any source radiating at a wavelength λ there is a near zone which extends to $\mu_* = \sqrt{\alpha/4\pi}\sqrt{\hbar c/G}$ In terms of the wave-vector the condition that makes this so is $\kappa \cdot r = 1$. The near zone is what is called the velocity field in the Li ĕ nard-Wiechert potentials.

The radius of the near zone scales inversely as the wave-vector. The larger the wave vector the smaller the near zone. Within the near zone the fields are Coulomb-like. The fields exert a radially outward pressure. At the edge of the near zone retardation sets in when the tangential velocity approaches the speed of light; fields acquire a transverse component; they propagate figure 2. An excellent animation of an accelerating charge and accompanying fields can be found in [7].

ftbpFU6.3918in4.1606in0ptCross section of fields from a charge after an external upward impulse. Figure 2 nearzone.pnglanguage "Scientific Word";type "GRAPHIC";maintain-aspect-ratio TRUE;display "USEDEF";valid_

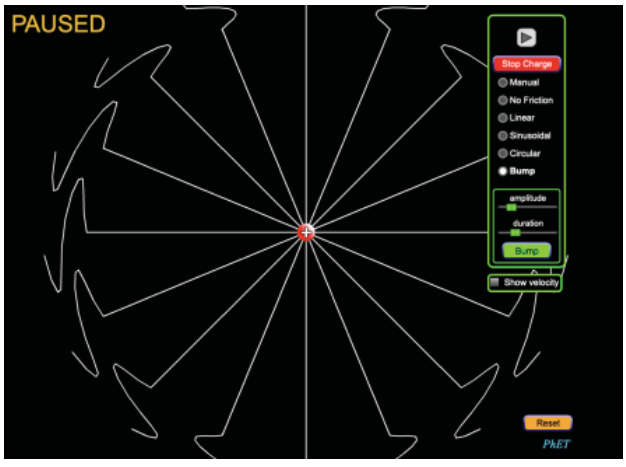

Figure 2 Simulation snapshot showing the trajectory pattern generated under the "Bump" mode in the PhET electric field simulation. The figure illustrates the radial motion and directional changes of the charged particle around the central source charge.

file "F";width 6.3918in;height 4.1606in;depth 0pt;original-width 21.0002in;original-height 13.639in;cropleft "0";croptop "1";cropright "1";cropbottom "0";filename 'NearZone.png';file-properties "XNPEU";

The fields can be divided into two classes. Radial field lines emerge from the charge. Further out radial lines segue into transverse fields due to retardation.

The two regions can be classified as radiating transverse fields and near zone radial fields. The lower limit of the $k-$ vector starts at the boundary between the two regions. The range of the $k-$ vector spans the near zone.

Increasing values $k-$vector sample inner regions. The energy density increases as r^{-4}. Increasing energy density engenders general relativistic effects. The result is an inward gravitational pressure which balances the outward radiation pressure. The two competing pressures stabilize the electron. Field energy is stored within the near zone. This energy manifests itself as an excess mass in Eq.(1.1). With an accelerating charge, energy is continuously exchanged between fields and source in the near zone; pictorially represented as the emission and absorption of single photons [?]. One consequence is the radiation reaction on the charge. Higher order diagrams correspond to quadrupole, octupole and higher order fields. Identifying this mechanism is the central concept of this paper.

Physical interpretation of the upper limit k in the integral Eq. (1.1: the wave vector k is proportional to the reciprocal of the wavelength λ, $k = \hbar(2\pi/\lambda) = \hbar/r$. Thus $k \propto 1/r$. As the upper limit increases the near zone radius shrinks with decreasing r. A decreasing radius implies an increase in the energy density $(\propto r^{-4})$. So as the upper limit increases it accesses regions of the near field with increasing energy density. If the upper limit $k \to \infty$, the energy density also $\to \infty$. As long as the upper limit is allowed to

acquire infinite value the integral will diverge. We discover that the divergence is built in to the theory. Reason why all efforts to normalize the integral to date have failed. The solution to this dilemma identifies the limit to the energy density. The energy density, or the pressure, is the stress tensor. The stress tensor exerts an inward pressure on the field in the near zone. If the stress tensor is high enough it becomes the source of a curved metric on the left hand side of the Einstein equation. The metric reacts against the field pressure. Until for some value of r the two opposing forces are equal. For this value of r the system - near field plus metric - is at equilibrium.

Gravitation

We can see how gravity comes into the picture. The energy density of an electron, for example, of radius r equal to a Compton wavelength (λ_C) can be estimated. Setting $r = \lambda_C$

$$\frac{e^2}{4\pi\epsilon_0 r}\frac{1}{(4\pi/3)r^3} = \frac{e^2}{4\pi\epsilon_0}\frac{3}{4\pi}\frac{1}{(\lambda_C)^4} = \frac{e^2}{4\pi\epsilon_0}\frac{3}{4\pi}\left(\frac{mc}{h}\right)^4 = 10^{18}\ J/m^3 \quad (2)$$

which is $\approx 10^{13}$ atmospheres; by comparison the pressure at the center of the Sun is 10^{11} atmospheres. This shows that such high energy densities are not just the purview of astrophysical sources but are common among elementary particles.

Clearly under these conditions energy densities are high enough to alter the metric in the vicinity of the electron. At these densities virtual excitations generate a curved metric. Virtual excitations loop back to the source along geodesics of the distorted metric. For example in figure 3 emission and absorption of virtual photons occurs in a curved metric. General relativistic effects not only cannot be ignored; they become essential part of the dynamics of the electron. Gravitation is intrinsic to the electron.

It is evident that theories that rely on flat space geometry are inadequate; the engendered divergences are evidence that in such theories a major reservoir of energy, the curved metric, is being ignored. The enormous outward forces cannot be balanced in flat space; curved space-time must be included.

There have been attempts to include gravity in QED phenomena. An early example is Isham, Salam and Strathdee, [8] and others.

Gravitating electron

In this paper we incorporate gravitation first by integrating Eq.(1.1) up to an upper limit for k . The upper limit is an unknown for now. We set the momentum

$$k = \hbar\kappa = \hbar\frac{2\pi}{\lambda} \quad (3)$$

where κ is the wave number. The corresponding near zone radius for λ is $r = \lambda/2\pi$.

Integrating Eq.(1.1) we get for the mass correction (see Appendix)

$$\Delta m \equiv \mu(\eta) = \frac{\alpha m}{2\pi}\left[-\frac{\eta}{2}\sqrt{1+\frac{1}{\eta}} + \eta + \ln\left\{\sqrt{\eta}\left(\eta\sqrt{1+\frac{1}{\eta}}+1\right)\right\}\right] \quad (4)$$

in terms of a dimensionless variable

$$\eta \equiv h/2mcr = \lambda_C/4\pi r \quad (5)$$

We have redefined $\Delta m \equiv \mu(\eta)$.

The energy density, or equivalently the stress tensor, alters the metric within the near zone. The net result is an inward pressure. Thus there are two competing pressures - an outward pressure from the field and an inward pressure from the metric. It is this balancing mechanism that stabilizes the electron.

Analogous to the Sun where the radiation pressure (or Fermi pressure in the case of white dwarfs or neutron stars) is balanced by the inward gravitational pressure.

As the upper limit of the $k-$ vector in Eq.(1.1) is increased, the stress tensor also increases, as well as the inward gravitation induced pressure.

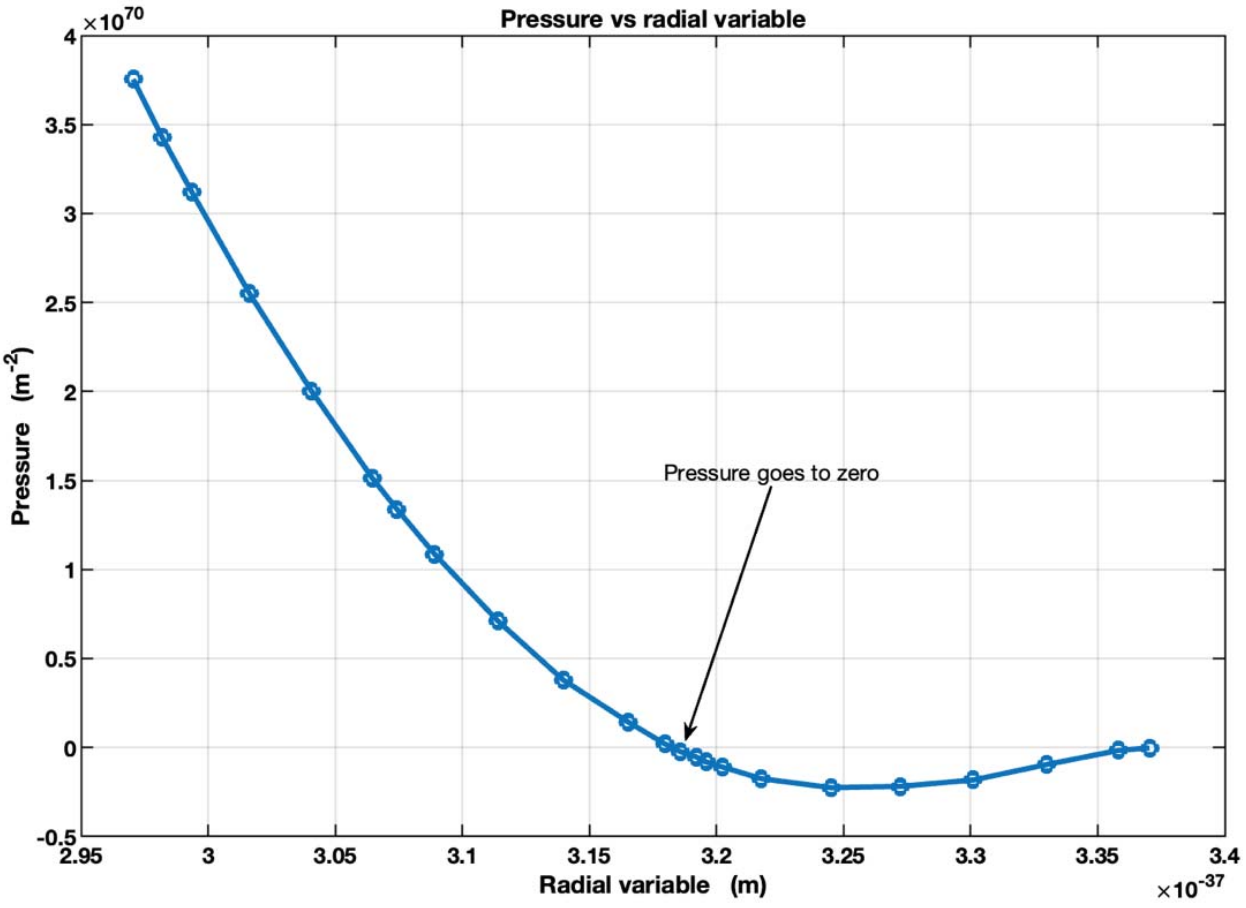

Figure 3 Variation of pressure with radial distance (rrr). The graph demonstrates the decrease in pressure as the radial variable increases, approaching zero near the critical radial position.

The electron is auto-stabilized.

Equating the two competing pressures yields an upper limit for k. We will calculate this limit.

In order to get an explicit condition for equilibrium we use the Einstein equation. We start with a line element of the form

$$ds^2 = e^{2\Phi}c^2dt^2 - e^{2\Lambda}dr^2 - r^2\left(d\theta^2 + \sin^2\theta\, d\phi^2\right) \quad (6)$$

Fields within the near zone are treated as those of a perfect fluid. Since there are no dissipative elements, the stress tensor of a perfect fluid has only diagonal elements. If there was dissipation, the electron would be unstable; it would decay to a lower energy state, which it does not. Furthermore in the rest frame, all momenta (off-diagonal elements) are zero.

The elements of the stress tensor are

$$T^{\hat{0}\hat{0}} = \rho; \quad T^{\hat{1}\hat{1}} = T^{\hat{2}\hat{2}} = T^{\hat{3}\hat{3}} = P \quad (7)$$

in the fluid's orthonormal rest-frame basis vectors. Imposing momentum conservation and spherical symmetry the relevant Einstein equations are

$$G^{\hat{0}\hat{0}} = \frac{e^{2\Phi-2\Lambda}\left(-1+e^{\Lambda}+2r\Lambda^2\right)}{r^2} = 8\pi T^{\hat{0}\hat{0}} = 8\pi\rho \quad (8)$$

$$G^{\hat{1}\hat{1}} = \frac{1-2e^{2\Lambda}+2r\, d\Phi/dr}{r^2} = 8\pi T^{\hat{1}\hat{1}} = 8\pi P \quad (9)$$

We define a new metric coefficient $\mu(r)$ (same as in Eq.(4) as

$$g_{11} = e^{2\Lambda} \equiv \frac{1}{1-\frac{2\mu(r)}{r}} \quad (10)$$

$\mu(r)$ is the corrected mass inside the radius r. The time-time component of Eq. (8), Eq. [6] takes the form

$$\frac{d\mu}{dr} = 4\pi r^2 \rho \tag{11}$$

whereas radial-radial component of Eq. (9), Eq. [6] takes the form

$$\frac{d\Phi}{dr} = 2\frac{\mu + 4\pi r^3 P}{r(r-2\mu)} \tag{12}$$

The proper density is

$$\rho = \frac{1}{4\pi r^2}\frac{1}{\sqrt{g_{11}}}\frac{d\mu}{dr} \tag{13}$$

Since the volume element

$$dV = \sqrt{|g_{11}|}r^2 \sin\theta \, d\theta \, d\phi \, dr \tag{14}$$

In terms of the dimensionless parameter η the density derivative is

$$\frac{d\rho}{d\eta} = \frac{d\rho}{dr}\frac{dr}{d\eta} \tag{15}$$

These equations when combined with the condition for hydrostatic equilibrium lead to the Tolman-Oppenheimer-Volkov equatio

$$\frac{dP(r)}{dr} = -\left(\rho(r) + P(r)\right)\frac{\left(\mu(r) + 4\pi r^3 P(r)\right)}{r^2\left(1 - \frac{2\mu(r)}{r}\right)} \tag{16}$$

This first order differential equation can be solved once the relation between pressure $P(r)$ and density $\rho(r)$ is established. The negative slope guarantees the decrease of $P(r)$ until for some value of r , $P(r) = 0$. We seek this value of r .

Equation of state

We can derive an equation of state of the radial field in the near zone (source of inertia) - relate $P(r)$ with $\rho(r)$. We use the work equation

$$dE = -P\,dV; \quad \frac{dE}{dV} = -P \tag{17}$$

Also $E = \rho V$thus

$$dE = V\,d\rho + \rho\,dV \tag{18}$$

$$\frac{dE}{dV} = \frac{d\rho}{dV}V + \rho = -P \tag{19}$$

$$\frac{d\rho}{dV} = \frac{d\rho}{dr}\frac{dr}{dV} = \frac{d\rho}{dr}\left(\frac{3}{4\pi}\right)^{1/3} V^{-2/3} \tag{20}$$

$$\frac{dE}{dV} = \frac{d\rho}{dr}\left(\frac{3}{4\pi}\right)^{1/3} V^{-2/3}V + \rho = -P \tag{21}$$

The near zone fields have an equation of state which is

$$P = -\rho - \frac{1}{3}r\frac{d\rho}{dr} \tag{22}$$

Or in terms of $\mu(r)$ the equation of state can be written as

$$P = -\frac{1}{4\pi r^2}\frac{1}{\sqrt{g_{11}}}\frac{d\mu}{dr} - \frac{1}{3}\frac{1}{4\pi r}\frac{1}{\sqrt{g_{11}}}\frac{d^2\mu}{dr^2} \tag{23}$$

Eq.(16) can be re-written in terms of the variable η.

$$\frac{dP}{d\eta} = \frac{dP}{dr}\frac{dr}{d\eta} \tag{24}$$

We calculate $P(\eta)$ by integrating $\frac{dP(\eta)}{d\eta}$

$$P(\eta) = \int \frac{dP(\eta)}{d\eta}d\eta \tag{25}$$

and find the root of the integral η_e for which $P(\eta_e) = 0$; this is the value of η and thus the lower limit r or the upper limit k we are looking for.

Results

In order to simplify the computation we will use an approximation where $\eta \gg 1$ to find the root of Eq.(16).

This allows us to simplify the terms $\mu(\eta)$, $\rho(\eta)$ and $P(\eta)$ (which has $\frac{\partial\rho}{\partial\eta}$).

For example for $\eta \gg 1$, $\rho(\eta)\to\frac{\eta^4}{2}$, $\frac{\partial\rho}{\partial\eta}\to 2\eta^3$, $\mu(\eta)\to\frac{\eta}{2}$. For the root η_e we get

$$\eta_e = 1.00255876\times\left(\frac{c^2}{2mG}\frac{2\pi}{\alpha}\frac{\hbar}{2mc}\right)^{1/2} = 1.00255876\times\frac{1}{m}\sqrt{\frac{\pi\hbar c}{2\alpha G}} \quad (26)$$

where $P(\eta_e)=0$.

From approximate calculations the corresponding electron radius is obtained from Eq.(5)

$$r \approx 3.884879\times10^{-37}\,m \quad (27)$$

or

$$r_e = \sqrt{\frac{\alpha}{4\pi}}\sqrt{\frac{\hbar G}{c^3}} = \sqrt{\frac{\alpha}{4\pi}}l_P \quad (28)$$

$$r_e = \sqrt{\frac{e^2G}{4\pi c^4}} \quad (29)$$

We note that what is called the Planck length l_P appears naturally. More precisely if instead we integrate Eq.(25) numerically, we find when $\eta_e = 1.000689253\times\frac{1}{m}\sqrt{\frac{\pi\hbar c}{\alpha G}}$. The radius is

$$r_e = 3.892139\times10^{-37}\,m \quad (30)$$

If we compare Eq.(30) with Eq.(27) we see that they are consistent.

The radius is independent of the electron mass m and $\hbar$ and is entirely in terms of fundamental constants e, G and c. Since it is a radius independent of the electron mass we re-write the radius as a universal radius r_* in terms of the Planck length as

$$r_* = \sqrt{\frac{\alpha}{4\pi}}l_P \quad (31)$$

In terms of energy

$$r_* = 10^{20}\,GeV \quad (32)$$

We can use the results of numerical integration to map the pressure profile as a function of the proper radial distance from the center of the electron. As shown in the figure below the pressure falls off within the near zone until it drops to zero at the surface, figure 3. The solution is reminiscent of the external metric of a charged black hole (Reissner-Nordstrom metric).

ftbpFU4.3552in2.7752in0optPressure in interior of electron in geometrical units m^{-2}. Figure 3 Pressure vs radial distancelanguage "Scientific Word";type "GRAPHIC";maintain-aspect-ratio TRUE;display "USEDEF";valid_file "T";width 4.3552in;height 2.7752in;depth 0pt;original-width 5.6723in;original-height 3.6037in;cropleft "0";croptop "1";cropright "1";cropbottom "0";tempfilename 'TF8WNU02.wmf';tempfile-properties "XPR";

One may ask if general relativity is valid at such short lengths. The existence of black holes and the cosmic background radiation offer evidence to the contrary.

If we substitute η_e from Eq.(26) into Eq.(4) we get a mass independent of the electron mass. We call it the universal mass μ_*.

$$\mu_* = \frac{1}{2}\sqrt{\frac{\alpha}{4\pi}\frac{\hbar c}{G}} = \frac{1}{2}\sqrt{\frac{\alpha}{4\pi}}m_P \quad (33)$$

in terms of the Planck mass m_P. The Planck mass also appears naturally.

Simplifying the result

$$\mu_* = \frac{1}{2}\sqrt{\frac{1}{4\pi}}\sqrt{\frac{e^2}{G}} \quad (34)$$

dependent on e and G alone and independent of $\hbar$ and c. Numerically

$$\mu_* \approx 10^{17}\,GeV \quad (35)$$

This result is remarkable for several reasons. Since μ_* is enormously larger than the physical mass m it cannot be the corrected

mass. Furthermore μ_* is independent of mass; it is solely in terms of the fundamental constants e and G. Since it depends on e^2 it is also independent of the sign of the charge. The inescapable conclusion is that the result is a general result applicable to all charged particles irrespective of the mass and sign of the charge. The claim applies only to stable charged particles i.e., electrons and protons and their anti-particle pairs.

Although our goal was to derive the corrected electron mass we have found instead a mass that applies to all charged stable particles. A possible interpretation is that μ_* is the universal mass.

These observations also apply to the radius r_* since it too is independent of mass, and is in terms of the fundamental constants G, c and e. The value of μ_* is close to the GUT energy $\left(10^{16}\ GeV\right)$ where it is conjectured that all forces except gravity merge. It would appear that all forces, including gravity, merge at $10^{17}\ GeV$. Since the merged or unified field depends only on e and G it would be consistent to call it the electrogravity field. Why the discrepancy between the heoretical energy and the measured energy ($0.5\ Mev$)? We will provide an explanation in the next section.

Since the electrogravity field energy is independent of $\hbar$ one may also conclude that the unified field is not quantized but is a continuum. This is a serendipitous result.

The universal mass is exact. The integral converges to an exact value. Physical laws remain unaltered.

The momentum upper limit is

$$k^{\max} = \frac{\hbar}{r_e} \tag{36}$$

We reiterate that this is a self-regulating mechanism since if k creeps up beyond $k^{\max}$ it engenders a proportional reaction from the metric such that the system reverts to a state of equilibrium. The equilibrium is stable.

At $r = 4\times10^{-37} m$ where the two competing pressures are equal; the pressures are

$$10^{79} m^{-2} \tag{37}$$

in geometric units, or $10^{123}\ N/m^2$ in standard units. Evidently the electron surface is highly stressed; the pressure is $\approx 10^{118}$ atmospheres on the surface. By comparison the pressure inside neutron stars is merely $\approx 10^{30}$ atmospheres.

At this value the outward pressure due to the energy density of self-interaction equals the inward pressure of the curved metric.

Pictorially, the distorted metric in the vicinity of the electron looks like this photo-representation (Figure 4).

ftbpFU4.3915 in 3.3408 in 0pt Pictorial representation of the metric enveloping an electron. The photo was taken through a clear baking dish filled with a shallow layer of water. A graph paper was glued underneath. A wire dipped on the surface simulates an electron. The distorted metric is evident. Figure 4 surfacetension-2.pnglanguage "Scientific Word";type "GRAPHIC";maintain-aspect-ratio TRUE;display "USEDEF";valid_file "F";width 4.3915in;height 3.3408in;depth

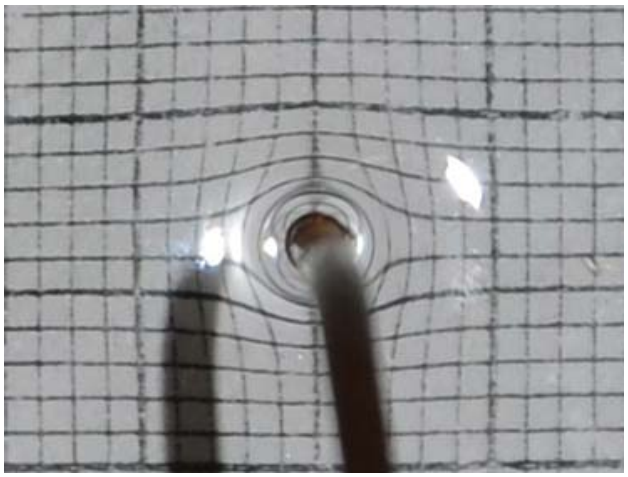

Figure 4 Experimental visualization of electric field line distortion around a cylindrical conductor placed on a conductive grid surface, showing the deformation of equipotential lines near the charged object.

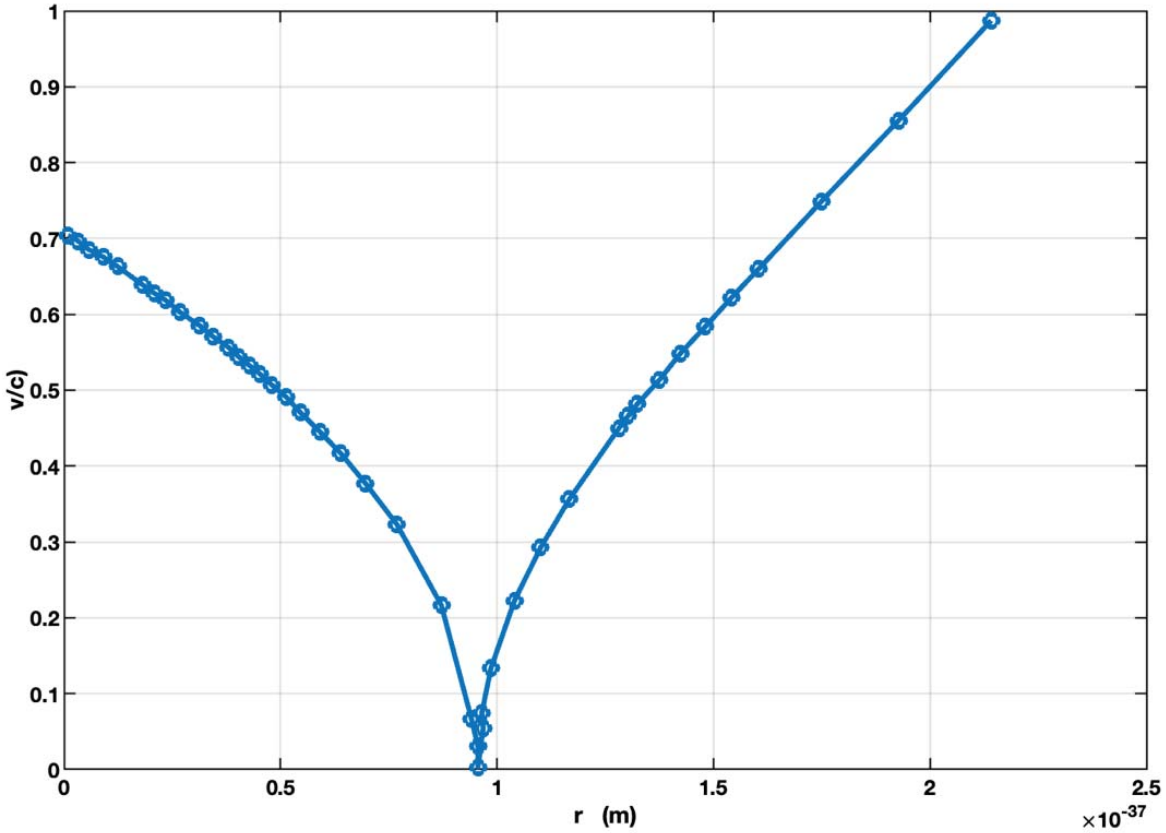

Figure 5 Graph of electric potential V(r)V(r)V(r) as a function of radial distance rrr. The potential decreases sharply near the central region and increases gradually away from the source.

opt;original-width 28.4618in;original-height 21.6151in;cropleft "0";croptop "1";cropright "1";cropbottom "0";filename 'C:/Users/mkari/OneDrive/Documents/SurfaceTension-2.png';file-properties "XNPEU";

The inward pressure is a consequence of the distorted metric.

Speed of Excitations

In this section we calculate the speed of excitations v within the electron. These are longitudinal excitations of the electrogravity field. Using Eq. (24) and Eq. (15)

$$\frac{v}{c}=\sqrt{\frac{dP/d\eta}{d\rho/d\eta}}$$

The graph in figure 5 shows v/c as a function of the proper distance r from the center. These are longitudinal waves within the near zone.

ftbpFU4.0491in3.614in0ptSpeed of excitations within the electron as a function of proper distance from center. Speed approaches c just below the surface. Figure 5v vs clanguage "Scientific Word";type "GRAPHIC";maintain-aspect-ratio TRUE;display "USEDEF";valid_file "T";width 4.0491in;height 3.614in;depth 0pt;original-width 3.9998in;original-height 3.5665in;cropleft "0";croptop "1";cropright "1";cropbottom "0";tempfilename 'TF8WNU03.wmf';tempfile-properties "XPR";

Discrepancy Between Theoretical and Measured Masses

In this section we resolve the apparent discrepancy between measured and theoretical values of the mass of electrons. The discrepancy is of the order of $10^{26}/0.511\times10^{6}\approx10^{21}$. The

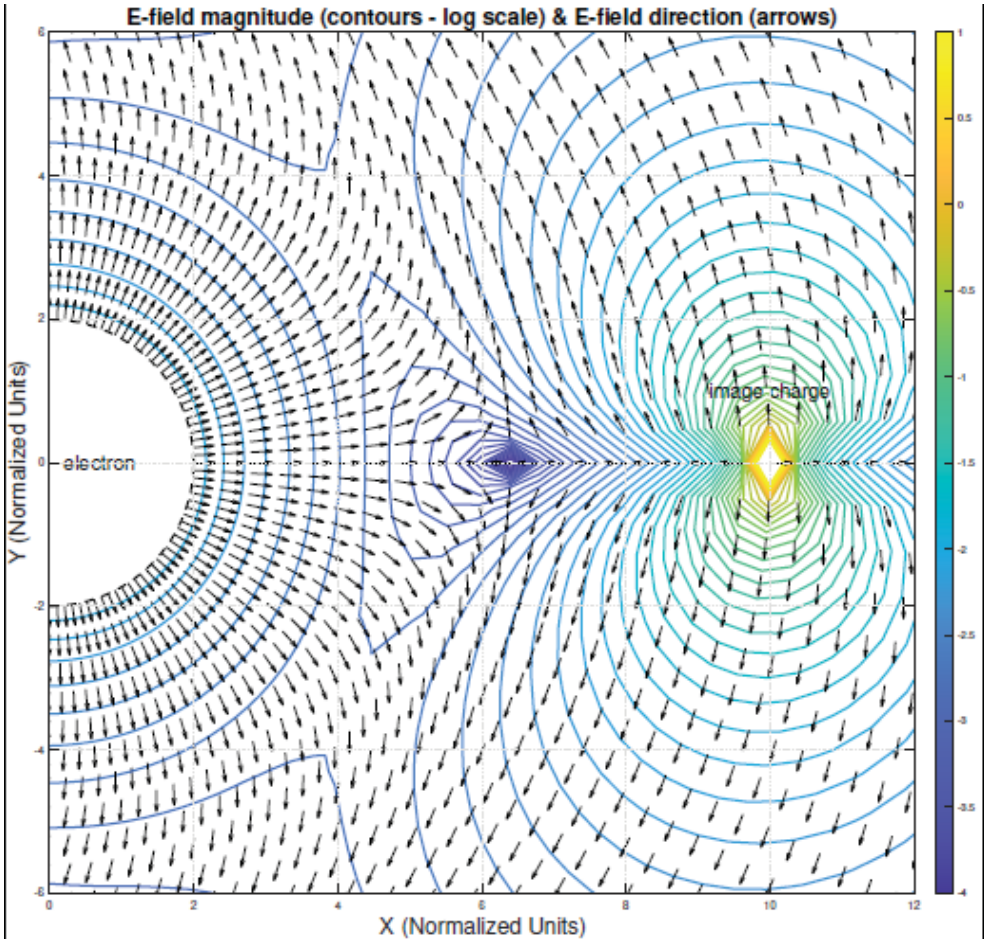

Figure 6 Electric field magnitude contours (log scale) and electric field direction vectors (arrows) illustrating the interaction between an electron and its image charge. The contour map represents field intensity distribution in normalized spatial coordinates.

measurement protocol entails a two-step process. Using the Thomson method we first measure the charge to mass ratio e/m then separately measure e using the Millikan oil drop method. The electron mass is calculated from the ratio of the two. In measuring e/m we rely on Thomson's experiment where an electron beam is launched into a region of uniform magnetic field. The acceleration associated with the Lorentz force on the moving electron is then equated to $F = ma$ from which the ratio e/m is calculated.

In the co-moving frame of the electron the magnetic field appears as an electric field E. The force on the charge e due to E is heavily reduced by the intervening metric surrounding the electron. We identify this mechanism which explains the discrepancy between theoretical and measured masses. Thus renormalization is neither necessary nor justified.; there is perfectly cogent explanation behind the discrepancy.

The external electric field (due to the co-moving frame) close to the surface of the electron can be calculated. We use the external field of a charged black hole - Reissner-Nordstrom metric to emulate the field of the electron, How is the external comoving field altered in a Riessner-Nordstrom metric?

We use results derived by Bini, Geralico and Ruffini [9]. Their work shows that the gravitational and electric fields interact, altering both - "electromagnetically induced

gravitational perturbation" as well as the "gravitational induced electromagnetic perturbation".

Using values typical in a Bainbridge e/m apparatus the E-field in the comoving frame of the circulating electron is $\approx 10^4 V/m$ at a distance of $0.1m$.

We can use the method of images to compute the location of an image charge. The image charge is at the center of the circle of the circulating electron beam.

Thus we achieve a geometry of an electron whose external field is represented by the Reissner-Nordstrom metric. The image charge and its electric field interacts with the electron. The geometry reproduces the model used in the paper referred to. We can use the results directly (Eqs. 14, 15 and 16) [9].

We find that the external electric field (due to the image charge, and indirectly due to the relative motion between electron and external magnetic field) is heavily attenuated in the vicinity of the electron. The result is a much smaller force and concomitant smaller acceleration.

The net effect is a much smaller measured electron mass when the ratio $e/(e/m)$ is calculated.

We show this explicitly. Denoting the external field by F_{ext}, the altered field as F_{th}, the experimental mass as m_{ex}, and the altered mass as m_{th} we may write the ratios

$$\frac{F_{ext}}{F_{th}} = \frac{m_{ex}\, a}{m_{th}\, a} \tag{38}$$

$$m_{th} = m_{ext}\frac{F_{th}}{F_{ext}} \tag{39}$$

ftbpFU5.2754in5.118in0pt Arrows of fields due to electron and image charge. Electron is on the left; image charge is within the diamond on the right. Field reversal is evident between location of the two charges. Figures 5,6 language "Scientific Word";type "GRAPHIC";maintain-aspect-ratio TRUE;display "USEDEF";valid_file "F";width 5.2754in;height 5.118in;depth 0pt;original-width 5.2191in;original-height 5.0626in;cropleft "0";croptop "1";cropright "1";cropbottom "0";filename 'C:/Users/mkari/OneDrive/Pictures/figure 5 tiff';file-properties "XNPEU";

In figure 6, we show the vector field graph of the electric fields from both the electron and the source charge in the external Reissner-Nordstrom metric of the electron. There are two source charges. The half disc on the left is the electron: the image charge appears as a diamond on the right. Clearly the field directions change sign in between. Near $r \approx 10^{-7} m$ the image field is close to zero or $\approx 10^{-21}$.

ftbpFU5.3368in4.1303in0optRatio of theoretical field vs. unaltered radial field. Figure 7, language "Scientific Word";type "GRAPHIC";maintain-aspect-ratio TRUE;display "USEDEF";valid_file "F";width 5.3368in;height 4.1303in;depth 0pt;original-width 5.2805in;original-height 4.0802in;cropleft "0";croptop "1";cropright "1";cropbottom "0";filename 'figure 6.png';file-properties "XNPEU";

In figure 6, we show a graph of the ratio of the theoretical field and the unaltered field against the radial coordinate. It shows the inflection point $(\log, r \approx -7.5)$ of the electric field at a precise location, corroborating what is in the vector field graph.

Conclusion

Although we have calculated the metric for electrons, we note that all stable particles with the same charge (e) have the same mass as well.

Previously there have been attempts to introduce gravitation to remove infinities in the self-energy correction to the electron mass [8], however, this work demonstrates the existence of

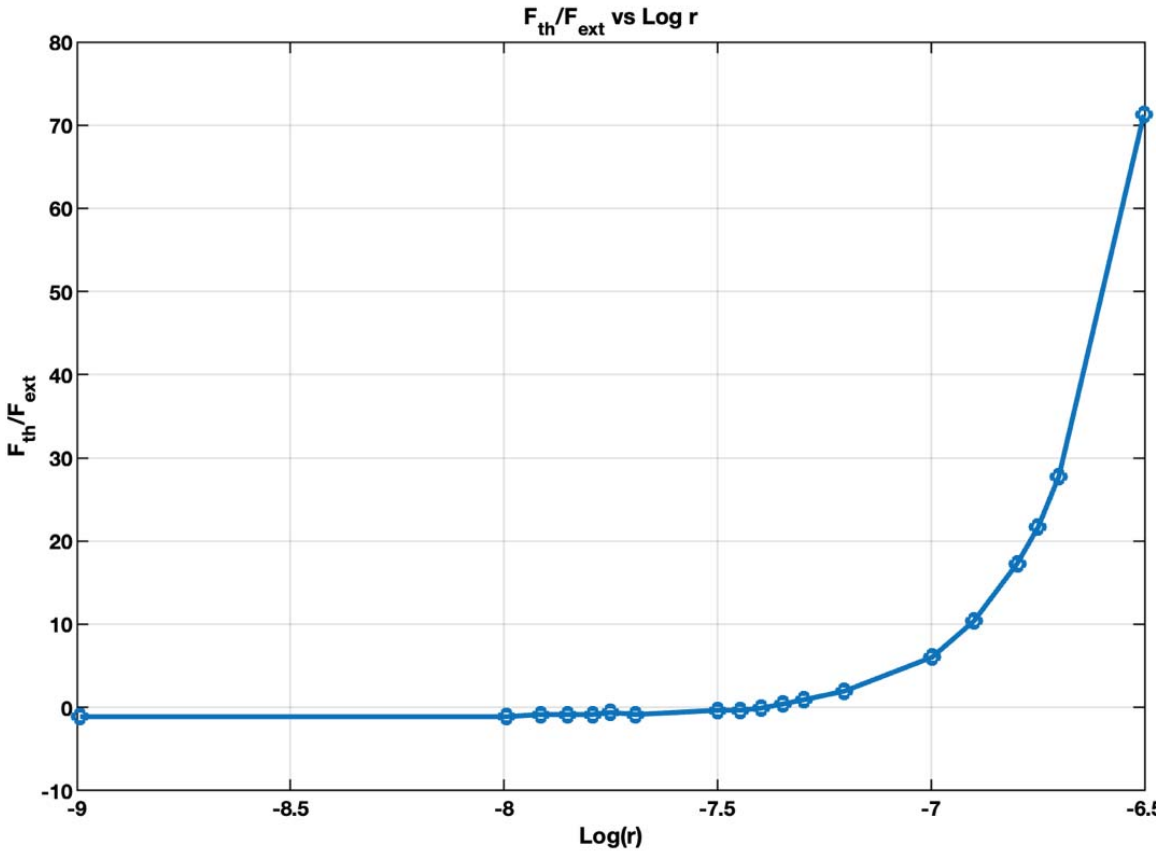

Figure 7 Relationship between electrostatic force (Fe/rF_{e/r}Fe/r) and logarithmic radial distance (log⁡r\log rlogr). The graph indicates a rapid increase in force magnitude as the radial separation decreases.

an auto-generated curved metric in the vicinity of an electron as well as an explicit computation of the upper limit on the momentum vector. The self-energy integral is shown to be finite; infinities in the perturbative expansion have been removed. The series converges. The mass correction has an exact value, free of infinities.

We have demonstrated that gravitation is essential to stabilize the electron. Gravitation is the beating heart of physics.

Competing pressures from the electromagnetic and gravitational fields auto-stabilize the electron. We have identified the Poincare' stress.

We calculate from first principles the radius of the electron as well as the Planck length and Planck mass. In deriving the electron radius and mass we identify the mechanism (inward pressure of the induced metric) that stabilizes the electron. The mass correction is close to the GUT scale - a serendipitous result.

We dispense with the theory that the electron is made up of a bare mass plus a radiative mass. It is evident that the electron is a stable configuration of the electrogravity field.

We have also demonstrated that the electrogravity field being independent of $\hbar$, is continuous. Furthermore, the fields merge at $10^{17} GeV$, consistent with the conjectured energy in Grand Unified Theories $\left(10^{16} GeV\right)$.

We have provided an explanation for the discrepancy of 10^{21} between measured and theoretical values of the electron mass.

We were able to calculate the speed of excitations of the electrogravity field within the

electron and discover that the internal structure is inhomogeneous - consisting of a hard shell enclosing a softer core.

Furthermore instead of using dimensional analysis to derive the Planck length and mass we show that both are a consequence of merging quantum electrodynamics with gravitation.

The solution we obtain is exact; since it is independent of mass it is valid for strong fields as well.

The first version of this paper was published in 2020 [10].

Acknowledgment

We are grateful to Mark Bocko for preparing the vector field graph ??, to Belal Baaquie who identified the connection between Eq.(28) and the Planck length, to Roberto Onofrio for continuous encouragement and advice, to the late Adrian Mellissinos for his interest in this work; and for support from my wife Maureen Patricia and daughter Kim Samar. A special thanks to Professors Habauka Kwaambwa and Percy Chimwamurombe for their continuing hospitality at the Namibia University of Science and Technology.

References

1. Thomson JJ. Cathode rays. Philos Mag. 1897;44(269):293-316. doi:10.1080/14786449708621070.
2. Poincaré H. Sur la dynamique de l'électron. C R Hebd Seances Acad Sci. 1905;140:1504-1508. Poincaré H. Sur la dynamique de l'électron. Rend Circ Mat Palermo. 1906;21:129-176. doi:10.1007/BF03013466.
3. Abraham M. Prinzipien der Dynamik des Elektrons. Ann Phys. 1903;315(1):105-179. doi:10.1002/andp.19023150105. Lorentz HA. Electromagnetic phenomena in a system moving with any velocity smaller than that of light. Proc R Neth Acad Arts Sci. 1904;6:809-831. Gralla SE, Harte AI, Wald RM. Rigorous derivation of electromagnetic self-force. Phys Rev D. 2009;80(2):024031. Wilczek F. Riemann-Einstein structure from volume and gauge symmetry. arXiv [Preprint]. 1998. Available from: arXiv:hep-th/9803075v2.
4. Bollini CG, Giambiagi JJ. Dimensional renormalization: The number of dimensions as a regularizing parameter. Nuovo Cim B. 1972;12:20-26. 't Hooft G, Veltman M. Regularization and renormalization of gauge fields. Nucl Phys B. 1972;44:189-213.
5. Feynman RP. Quantum Electrodynamics. Reading (MA): Addison-Wesley; 1962.
6. Adler RJ, Bazin M, Schiffer M. Introduction to General Relativity. 2nd ed. New York: McGraw-Hill; 1975. p. 466.
7. University of Colorado Boulder. Radiating Charge [Internet]. PhET Interactive Simulations; [cited 2026 May 22].
8. Isham CJ, Salam A, Strathdee J. Nonlinear realizations of space-time symmetries. Phys Rev D. 1971;3(8):1805-1817. Isham CJ, Salam A, Strathdee J. F-dominance of gravity. Phys Rev D. 1972;5:2548-2565.
9. Hanni RS, Ruffini R. Lines of force of a point charge near a Schwarzschild black hole. Phys Rev D. 1973;8:3259-3265. Bini D, Geralico A, Ruffini R. Charged massive particle at rest in the field of a Reissner-Nordström black hole. Phys Lett A. 2007;360:515-517. Bini D, Geralico A, Ruffini R. Electromagnetic field lines around black holes. arXiv [Preprint]. 2014. Available from: arXiv:1408.4591v1 [gr-qc].
10. Karim M. Int J Mod Phys A. 2020;35(2-3).6.2